

**Theoretical Limitations of the Elastic Wave Equation Inversion for Tissue  
Elastography**

Ali Baghani,<sup>a)</sup> Septimiu Salcudean, and Robert Rohling<sup>b)</sup>

*Department of Electrical and Computer Engineering,  
University of British Columbia*

*Kaiser Bldg,  
2332 Main Mall,  
Vancouver,  
BC,  
V6T 1Z4,  
Canada.*

## Abstract

This article examines the theoretical limitations of the local inversion techniques for the measurement of the tissue elasticity. Most of these techniques are based on the estimation of the phase speed or the algebraic inversion of a 1D wave equation. To analyze these techniques, the wave equation in an elastic continuum is revisited. It is proven that in an infinite medium, harmonic shear waves can travel at any phase speed greater than the classically known shear wave speed,  $\sqrt{\mu/\rho}$ , by demonstrating this for a special case with cylindrical symmetry. Hence in addition to the mechanical properties of the tissue, the phase speed depends on the geometry of the wave as well. The elastic waves in an infinite cylindrical rod are studied. It is proven that multiple phase speeds can coexist for a harmonic wave at a single frequency. This shows that the phase speed depends not only on the mechanical properties of the tissue, but also on its shape. The final conclusion is that the only way to avoid theoretical artifacts in the elastograms obtained by the local inversion techniques is to use the shear wave equation as expressed in the curl of the displacements, i.e. the rotations, for the inversion.

PACS numbers: 43.80.Ev, 43.80.Jz, 43.80.Vj, 43.80.Qf.

## I. INTRODUCTION

Elastography is a fast developing field of medical imaging which strives to provide images of the mechanical properties of tissue<sup>1-8</sup>. The main mechanical property of interest is the elasticity or Young's modulus  $E$ . Other mechanical properties of interest include viscosities, relaxation times, nonlinearity parameters, harmonics, poro-elasticity and Poisson's ratio<sup>8-22</sup>.

The majority of the elastography techniques have three components in common:

- an *excitation mechanism* which creates quasi-static or dynamic deformations in the tissue<sup>23-31</sup>,
- a medical imaging system augmented by a *motion estimation technique* which is capable of providing displacement (or velocity) images of the tissue while it is being deformed<sup>25,32-41</sup>, and
- an *inversion technique* which transforms the displacement images into elasticity images, the so called elastograms<sup>25,42-54</sup>.

For the inversion, different approaches have been devised. Most of them, however, fall under one of the two following categories:

- Global inversion techniques<sup>44-48,55-57</sup>: These techniques typically use finite element modeling (FEM) of the medium. The goal is to find the best local elasticity values which would create the same displacement pattern as those observed inside the tissue, under similar boundary and excitation conditions. To find the optimum elasticity values, the forward problem is solved iteratively. In each iteration the elasticity values are adjusted until the computed displacements from the model match the measured displacement from the tissue. In addition to the measured displacements, these techniques typically require further information about the shape of the tissue, its boundary conditions, and the excitation.

---

<sup>a)</sup>Electronic mail: [baghani@ece.ubc.ca](mailto:baghani@ece.ubc.ca)

<sup>b)</sup>Also at Department of Mechanical Engineering, University of British Columbia

- Local inversion techniques<sup>11,25,27–30,37,50–52,58–61</sup>: Typically in these techniques, a particular *wave equation* is assumed to govern the displacements. This partial differential equation (PDE) relates the spatial derivatives to the temporal derivatives of the displacement with the local elasticity as the coefficient. If the displacement measurements are available over a range of space and time, the elasticities can be found either by an algebraic inversion of the wave equation or by estimating the phase speed from the gradient of the phase. The next section is devoted to the presentation of these techniques.

It is the objective of this research to:

- Study the theoretical limitations of the local inversion techniques for estimating the tissue elasticity.
- Study the effects of the formulation of the wave equation on the inversion results.
- Study the effects of the choice of the exciter and imaging technique.

To this end, the general form of the elastic wave equation in a linear continuum is studied. The hypothesis to be proven is that the *phase speed*, which is the final estimated quantity in many of the local inversion techniques, does not exactly represent the local mechanical properties of the tissue. The hypothesis is proven by showing that in addition to the local mechanical properties of the tissue, the phase speed depends on the geometry of the wave as well as the geometry of the tissue itself. This effect is known as the Lamb wave effect specially in the context of thin plates<sup>62</sup>. The practical implication is that artifacts are inevitably present in the elastograms, no matter how well the algorithm is implemented or how accurate the displacement measurements are. Nevertheless, many of the elastography techniques have been proven clinically to provide valuable information about the elasticity of the tissue. The excitation in these techniques is chosen so that the actual displacements created in the tissue satisfy the assumptions made, which in turn justifies the inversion techniques used. These methods include quasi-static constant strain compression, pulsed excitation with external exciters, and acoustic-radiation-force-based techniques.

A previous study of the limitations of the local inversion techniques for estimating the tissue elasticity can be found in<sup>63</sup>. In that work the authors experimentally measured the displacements caused by a circular piston inside rectangular blocks of tissue mimicking material and meat specimens. In their experiments the exciter would start to vibrate at a single frequency (monochromatic excitation). Between the transient and steady state regimes of vibration, a region was identified when transient shear waves are propagating in the medium and phase speed measurements can be carried out. The deleterious effects of the medium boundaries were dealt with by rejecting the steady state regime for phase speed measurements. The effects of the boundary conditions imposed by the exciter were also studied. An approximate model, the Rayleigh–Sommerfeld’s solution, and the Green’s function were used in this analysis. They concluded that the size of the exciter affects the measured phase speed. Another conclusion was that at very low frequencies, the effects of the longitudinal wave on the phase speed cannot be neglected. The final preferred method was to use a pulsed transient excitation with a small piston to get more accurate viscoelastic measurements.

The analysis of the aforementioned article is limited to the particular configuration used, which is very similar to a point source on a semi-infinite medium. In many elastography applications, to get a desired level of displacements inside tissue, it is of interest to use exciters with a larger footprint. We have shown previously that if the size of the exciter is comparable to the size of the sample, the phase speed observed is the extensional wave speed<sup>64</sup>. In the present article we look at the problems associated with phase speed measurements from a more general point of view, and discuss some of the phenomena that affect the accuracy of the measurements. We will show that neglecting these phenomena results in un-accounted-for artifacts in the computed elastograms.

We start by a brief review of the state-of-the-art local inversion techniques in Section II. Section III is a critique on the use of the terminology associated with the elastic waves. The main theoretical results of the article are presented in Section IV. Simulation results are presented in Section V. Section VI is devoted to the conclusion.

## II. LOCAL INVERSION OF THE WAVE EQUATION

The mechanical wave equation in an isotropic elastic continuum written in the Cartesian coordinate system is<sup>62</sup>

$$\rho \frac{\partial^2 u_i}{\partial t^2} = (\lambda + \mu) \frac{\partial}{\partial i} \Delta + \mu \nabla^2 u_i \quad i = x, y, z, \quad (1)$$

where  $\mathbf{x} = [x, y, z]^T$  are the Cartesian coordinates which define the spatial location of the point,  $t$  is the time variable,  $\mathbf{u}(\mathbf{x}, t) = [u_x, u_y, u_z]^T$  is the displacement field, and the coefficients  $\rho(\mathbf{x})$ ,  $\lambda(\mathbf{x})$  and  $\mu(\mathbf{x})$  are the density, the first, and the second Lamé constants respectively. Here, we have adopted the notation of Kolsky<sup>62</sup>. The dilatation  $\Delta$  is defined by

$$\Delta = \frac{\partial u_x}{\partial x} + \frac{\partial u_y}{\partial y} + \frac{\partial u_z}{\partial z}, \quad (2)$$

and determines the voluminal changes as the wave propagates.  $\nabla^2$  is the Laplacian operator:

$$\nabla^2 = \frac{\partial^2}{\partial x^2} + \frac{\partial^2}{\partial y^2} + \frac{\partial^2}{\partial z^2}. \quad (3)$$

We denote the Poisson's ratio and the Young's modulus by  $\nu$  and  $E$  respectively.

The material of interest in the field of elastography is tissue *in vivo*. This material is found to be nearly incompressible<sup>51,65</sup>, hence the values of  $\Delta$  are typically very small. Other implications of the incompressibility in terms of the mechanical properties are as follows:

$$\nu \approx 0.5 \quad , \quad \lambda \gg \mu \quad \text{and} \quad E \approx 3\mu. \quad (4)$$

In the rest of this article it is assumed that the relations (4) hold.

To obtain a clinically useful image of the soft tissue, the contrast should be based on a physical quantity which has a high degree of variability among different tissue types. The density of most soft tissue is close to the density of water<sup>66</sup>, 1000kg/m<sup>3</sup> so  $\rho$  is not a candidate. Neither is the first Lamé constant  $\lambda$  which is found to be close to the  $\lambda$  of water<sup>67</sup>, *i.e.* 2.3GPa. On the other hand,  $\mu$  and  $E = 3\mu$ , which determine the stiffness of the tissue, vary over a wide range from a few to a few hundred kPa<sup>68</sup>. Moreover, a change in the stiffness of the tissue is often associated with pathology<sup>69-71</sup>. Hence elastograms are

preferentially based on the tissue elasticity  $E = 3\mu$ . Given the displacements as a function of time and space, the most that can be recovered from equation (1) are the ratios  $\lambda/\rho$  and  $\mu/\rho$ . In practice, the elastograms are based on  $E/\rho$ . Since the variability of  $\rho$  is small, the obtained contrast is almost the same as the one obtained by using the absolute value of elasticity  $E$ .

A number of issues arise when medical imaging devices are used to estimate the displacement fields. In many cases it is not possible to acquire all three components of the displacement field, i.e.  $u_x$ ,  $u_y$ , and  $u_z$ . In other cases the acquired displacement field may not be available over a volume. For instance, in most cases of ultrasound elastography with 2D probes, only  $u_x(x, y)$  is available and only on a single plane  $z = \text{constant}$  and not over a volume. Some customized ultrasound systems can estimate the displacements over a volume and in multiple directions<sup>37,41,72</sup>. MRI based techniques on the other hand, can acquire the full displacement field over a volume, at the expense of longer acquisition times<sup>14,25,50,51,73–75</sup>.

Different approaches to the inversion of the wave equation have been taken. As mentioned earlier the dilatation  $\Delta(\mathbf{x}, t)$  levels in soft tissue are well beyond the accuracy of the measurement systems. Therefore the wave equation (1) cannot directly be inverted to obtain  $\mu/\rho$ . Some state-of-the-art approaches to tackle this problem are as follows:

- Assuming zero dilatation or zero pressure gradient<sup>30,36,37,58,59</sup>: In this approach it is assumed that the dilatation is identically zero,  $\Delta \equiv 0$ , or that the pressure has no spatial variation in the medium. These assumptions reduces the wave equation to

$$\rho \frac{\partial^2 u_i}{\partial t^2} = \mu \nabla^2 u_i \quad i = x, y, z. \quad (5)$$

Note that for an anisotropic inversion all three components are necessary. If isotropy is assumed, measuring one component of the displacement field, for instance  $u_x$ , is enough. In this case, it is natural to chose the measurement axis (the  $x$ -axis) aligned with the axis on which the wave causes the greatest displacements. If the measurement is only available on a plane, for instance  $u_x(x, y)$ , or on a single line,  $u_x(x)$ , then the

following assumptions are usually made

$$\begin{aligned}\nabla^2 u_x &= \left( \frac{\partial^2}{\partial x^2} + \frac{\partial^2}{\partial y^2} + \frac{\partial^2}{\partial z^2} \right) u_x \\ &\approx \left( \frac{\partial^2}{\partial x^2} + \frac{\partial^2}{\partial y^2} \right) u_x \\ &\approx \frac{\partial^2}{\partial x^2} u_x.\end{aligned}\tag{6}$$

- Assuming a shear wave equation<sup>52</sup>: In this case it is assumed that the wave is a plane shear wave. If the wave causes the greatest displacements in the  $x$ -direction, then this component of the displacement field is measured and assumed to satisfy a 1D shear wave equation,

$$\rho \frac{\partial^2 u_x}{\partial t^2} = \mu \frac{\partial^2 u_x}{\partial y^2}.\tag{7}$$

- Assuming a thin rod (extensional) wave equation<sup>64</sup>: When the size of a compressing exciter is comparable to the dimensions of the tissue being imaged the tissue behaves like a thin rod experiencing extensional waves. Under these conditions the component of the displacement field parallel to the direction of the excitation, say the  $x$ -component, satisfies

$$\rho \frac{\partial^2 u_x}{\partial t^2} = E \frac{\partial^2 u_x}{\partial x^2}.\tag{8}$$

- Writing the shear wave equation for the rotations<sup>14,53,72-75</sup>: Define the rotation  $\mathbf{w}(\mathbf{x}, t)$  as half the curl of the displacement field:

$$\mathbf{w}(\mathbf{x}, t) = \frac{1}{2} \nabla \times \mathbf{u}(\mathbf{x}, t)\tag{9}$$

From (1) each component of the rotation field satisfies a separate shear wave equation,

$$\rho \frac{\partial^2 w_i}{\partial t^2} = \mu \frac{\partial^2 w_i}{\partial i^2} \quad i = x, y, z.\tag{10}$$

Note that this approach does not make any assumptions, but it requires the measurement over a 3D volume of at least two components of the displacement field for an isotropic inversion. For an anisotropic inversion, all the components are necessary.

The local inversion algorithms (with the exception of the last approach) reduce the general form of the wave equation (1) to a 1D wave equation of the form

$$\rho \frac{\partial^2 u_x}{\partial t^2} = f(E) \frac{\partial^2 u_x}{\partial x^2}, \quad (11)$$

where  $f(E)$  is a function of the local elasticity. The quantity

$$c_{ph} = \sqrt{f(E)/\rho} \quad (12)$$

in this 1D equation is called the *phase speed*. For a unidirectional harmonic solution,

$$u_x(x, t) = a \exp(j\omega(x/c_{ph} - t)), \quad (13)$$

this quantity gives the propagation speed of the constant phase surfaces.

Given  $u_x(x, t)$ , it is possible to invert equation (11) and find  $f(E)/\rho$ . This can be done either by directly solving for  $f(E)/\rho$ :

$$\frac{f(E)}{\rho} = \frac{\partial^2 u_x / \partial t^2}{\partial^2 u_x / \partial x^2}, \quad (14)$$

This method is sometimes called the Algebraic Inversion of the Differential Equation (AIDE)<sup>50</sup>. Another method is to use the concept of the phase speed,

$$\sqrt{f(E)/\rho} = c_{ph} = \frac{\omega}{\frac{\partial}{\partial x} \angle u_x}, \quad (15)$$

sometimes called the Phase Gradient method<sup>50</sup>.

If  $f(E)$  were only a function (even an unknown function) of the local mechanical properties of the tissue, the elastograms based on the phase speed,  $\sqrt{f(E)/\rho}$  would be free from artifacts. However as we show in Section IV,  $f(E)$  is not only a function of the local mechanical properties of the medium but also a function of the geometry of the wave and the geometry of the medium. An even more important result is proved; the reduction of (1) to (11) may not be possible at all since multiple values of the phase speed can coexist.

### III. A CRITIQUE ON THE TERMINOLOGY ASSOCIATED WITH THE WAVE EQUATION

Before we move on to our results on the phase speed we present our choice of the terminology. By the fundamental theorem of vector calculus, or Helmholtz decomposition theorem, any sufficiently smooth and decaying vector field can be written as the sum of a divergence-free and a curl-free vector field<sup>76</sup>. The solutions of the wave equation (1) satisfy the conditions of the theorem, and therefore it is possible to write a vibration pattern inside an elastic medium as the sum of a divergence-free and a curl-free displacement field.

- *Dilatational wave*: or better termed *irrotational component* is a component of the wave which is curl-free. This component of the wave phenomena is solely the result of voluminal changes in the medium.
- *Distortion wave*: or better termed *equivoluminal component* is a component of the wave which is divergence-free. This component of the wave phenomena preserves the volumes of the infinitesimal elements.

There is some confusion however, over the definition and application of the terms “shear wave”, “transverse wave”, “longitudinal wave” , and “compressional wave”. These terms are sometimes defined as follows:

- *Longitudinal wave*: or *compressional wave* is a wave for which the particle velocities are parallel to the phase velocity. For a harmonic wave the particle velocity would be perpendicular to the equiphase surfaces.
- *Transverse wave*: or *shear wave* is a wave for which the particle velocities are perpendicular to the phase velocity. For a harmonic wave the particle velocity would be tangent to the equiphase surfaces.

These definitions are very intuitive with respect to the literal meanings of the terms. However a major problem exists with these definitions; to the best knowledge of the authors, there

is no theorem proving that the quality of a wave being transversal or longitudinal (taken these definitions) is invariant with respect to the wave equation. In other words, a wave propagating in an infinite elastic medium might be purely longitudinal at one instant but not so at a later instant (even without encountering a boundary and undergoing mode conversion). This severely limits the applicability of these terms.

When these definitions are taken, a connection is usually assumed between longitudinal and irrotational waves on one hand and transverse and equivoluminal waves on the other hand. The origin of this connection could be the study of the simple case of a plane wave in an infinite medium. Indeed a longitudinal plane wave propagating in an infinite medium has no equivoluminal components and consists solely of a dilatational component. This wave propagates at a phase speed of  $\sqrt{(\lambda + 2\mu)/\rho}$  hence the name *longitudinal wave speed*. Similarly a shear plane wave propagating in an infinite medium has no dilatational components and consists solely of an equivoluminal component. This wave propagates at a phase speed of  $\sqrt{\mu/\rho}$  hence the name *shear wave speed*.

A better way to define these terms, however, is to take for them the same definitions as presented for the “dilatational waves” and “distortion waves”. This is the accepted nomenclature in the physics literature, specially in the field of the electromagnetic waves<sup>77</sup>:

- *Longitudinal wave*: or *compressional wave* is a component of the wave which is curl-free.
- *Transverse wave*: or *shear wave* is a component of the wave which is divergence-free.

These are the definitions we use in this article and recommend.

A number of comments are in order. It is clear from the definitions that a wave can contain both the longitudinal and transversal components, or may lack one. In some cases one is not interested in the decomposition of the displacement field into these components, but rather in the study of the total displacement itself. However since each of these components separately satisfies a reduced wave equation with a definite wave speed, it is at other times useful to study them separately. The speed of the longitudinal component and the

transverse component is equal to  $\sqrt{(\lambda + 2\mu)/\rho}$  and  $\sqrt{\mu/\rho}$  respectively.

Since the wave equation can be reduced to the two aforementioned wave equations, it is evident that in an infinite elastic medium, a purely longitudinal wave will remain purely longitudinal, and a purely transverse wave will remain purely transverse. This invariance property make the terms well-defined. The drawback is that the intuitive relationship between the directions of the particle velocity and the phase velocity is no longer valid. As a matter of fact, the quality of a wave being longitudinal or transversal could be determined solely from the displacement vector field at a single instant. The wave equation preserves this quality as the time evolves.

As will become clear in the next section, the relationship between the phase speed and the longitudinal and shear wave speeds,  $\sqrt{(\lambda + 2\mu)/\rho}$  and  $\sqrt{\mu/\rho}$ , is a complex relationship which depends on the geometry of the wave, as well as the geometry of the medium.

## IV. PHASE SPEED OF MECHANICAL WAVES IN ELASTIC MEDIUMS

### A. Dependence of the Phase Speed on the Geometry of the Wave: Infinite Mediums

**Theorem.** *Consider an infinite homogeneous linear elastic medium with density  $\rho$  and Lamé constants  $\lambda$  and  $\mu$ . Given the angular frequency  $\omega$  for a harmonic wave:*

- *for any number  $c$  such that*

$$\sqrt{\frac{\mu}{\rho}} \leq c < \sqrt{\frac{\lambda + 2\mu}{\rho}}, \quad (16)$$

*there exists a shear beam form for the harmonic wave for which the phase speed is equal to  $c$ .*

- *for any number  $c$  such that*

$$\sqrt{\frac{\lambda + 2\mu}{\rho}} \leq c, \quad (17)$$

*there exists infinitely many beam forms for the harmonic wave for which the phase speed is equal to  $c$ . These waves contain both longitudinal and shear components.*

The theoretical derivation which follows can be found in classical textbooks on elastic waves<sup>62,78</sup> as part of the solution to the wave equation in cylindrical coordinate systems. However studying the implications in terms of the phase speed, as summarized in the theorem, is novel.

*Proof.* Consider the elastic wave equation in the cylindrical coordinate system,

$$\rho \frac{\partial^2 u_r}{\partial t^2} = (\lambda + 2\mu) \frac{\partial \Delta}{\partial r} - \frac{2\mu}{r} \frac{\partial \bar{\omega}_z}{\partial \theta} + 2\mu \frac{\partial \bar{\omega}_\theta}{\partial z}, \quad (18)$$

$$\rho \frac{\partial^2 u_\theta}{\partial t^2} = (\lambda + 2\mu) \frac{1}{r} \frac{\partial \Delta}{\partial \theta} - 2\mu \frac{\partial \bar{\omega}_r}{\partial z} + 2\mu \frac{\partial \bar{\omega}_z}{\partial r}, \quad (19)$$

$$\rho \frac{\partial^2 u_z}{\partial t^2} = (\lambda + 2\mu) \frac{\partial \Delta}{\partial z} - \frac{2\mu}{r} \frac{\partial}{\partial r} (r \bar{\omega}_\theta) + \frac{2\mu}{r} \frac{\partial \bar{\omega}_r}{\partial \theta}, \quad (20)$$

where  $(r, \theta, z)$  are the cylindrical coordinates and  $u = (u_r, u_\theta, u_z)$  is the displacement field.

The dilatation in the cylindrical coordinates is given by,

$$\Delta = \frac{1}{r} \frac{\partial}{\partial r} (r u_r) + \frac{1}{r} \frac{\partial u_\theta}{\partial \theta} + \frac{\partial u_z}{\partial z}, \quad (21)$$

and the rotations are given by,

$$2\bar{\omega}_r = \frac{1}{r} \frac{\partial u_z}{\partial \theta} - \frac{\partial u_\theta}{\partial z}, \quad (22)$$

$$2\bar{\omega}_\theta = \frac{\partial u_r}{\partial z} - \frac{\partial u_z}{\partial r}, \quad (23)$$

$$2\bar{\omega}_z = \frac{1}{r} \left[ \frac{\partial}{\partial r} (r u_\theta) - \frac{\partial u_r}{\partial \theta} \right]. \quad (24)$$

Consider a cylindrical wave beam propagating along the  $z$ -axis with the center of the beam on the  $z$ -axis. More specifically assume that  $u_\theta$  is zero, *i.e.* the particle displacements are confined to the  $rz$ -planes. Also assume that the wave is symmetrical around the  $z$ -axis, hence  $\partial/\partial\theta$  annihilates the variables. From (22) and (24)  $\bar{\omega}_r = \bar{\omega}_z = 0$ . The reduced wave equation in this case would be,

$$\rho \frac{\partial^2 u_r}{\partial t^2} = (\lambda + 2\mu) \frac{\partial \Delta}{\partial r} + 2\mu \frac{\partial \bar{\omega}_\theta}{\partial z}, \quad (25)$$

$$\rho \frac{\partial^2 u_z}{\partial t^2} = (\lambda + 2\mu) \frac{\partial \Delta}{\partial z} - \frac{2\mu}{r} \frac{\partial}{\partial r} (r \bar{\omega}_\theta). \quad (26)$$

We are interested in harmonic waves propagating along the  $z$ -axis, for instance in the negative  $z$ -direction. The general form of such a wave is,

$$u_r = U(r) \exp(i(k_z z + \omega t)) , \quad (27)$$

$$u_z = W(r) \exp(i(k_z z + \omega t)) , \quad (28)$$

where  $k_z$  is the wave number and  $\omega$  is the angular frequency.  $U(r)$  and  $W(r)$  determine the shape of the beam. Note that the phase speed of this wave is equal to  $c_{ph} = \omega/k_z$ .

Substitution in (21) and (23) yields the expressions for the dilatation and rotation:

$$\begin{aligned} \Delta(r, z, t) = & \\ & \left[ \frac{\partial U(r)}{\partial r} + \frac{U(r)}{r} + ik_z W(r) \right] \exp(i(k_z z + \omega t)) , \end{aligned} \quad (29)$$

$$\begin{aligned} 2\bar{\omega}_\theta(r, z, t) = & \\ & \left[ ik_z U(r) - \frac{\partial W(r)}{\partial r} \right] \exp(i(k_z z + \omega t)) . \end{aligned} \quad (30)$$

The forms (27) and (28) simplify the wave equation (25) and (26),

$$-\rho\omega^2 u_r = (\lambda + 2\mu) \frac{\partial \Delta}{\partial r} + 2i\mu k_z \bar{\omega}_\theta , \quad (31)$$

$$-\rho\omega^2 u_z = ik_z (\lambda + 2\mu) \Delta - \frac{2\mu}{r} \frac{\partial}{\partial r} (r\bar{\omega}_\theta) . \quad (32)$$

By eliminating  $\bar{\omega}_\theta$  and  $\Delta$  between these equations, the longitudinal and transversal wave equations are derived:

$$\frac{\partial^2 \Delta}{\partial r^2} + \frac{1}{r} \frac{\partial \Delta}{\partial r} + k_\Delta^2 \Delta = 0 , \quad (33)$$

$$\frac{\partial^2 \bar{\omega}_\theta}{\partial r^2} + \frac{1}{r} \frac{\partial \bar{\omega}_\theta}{\partial r} - \frac{\bar{\omega}_\theta}{r^2} + k_{\bar{\omega}_\theta}^2 \bar{\omega}_\theta = 0 , \quad (34)$$

where  $k_\Delta$  and  $k_{\bar{\omega}_\theta}$  are the geometrical beam numbers defined by

$$k_\Delta^2 = \frac{\omega^2}{\frac{\lambda+2\mu}{\rho}} - k_z^2 , \quad (35)$$

$$k_{\bar{\omega}_\theta}^2 = \frac{\omega^2}{\frac{\mu}{\rho}} - k_z^2 . \quad (36)$$

In the case that the desired phase speed,  $c$ , satisfies (16) the corresponding choice of the wave number,

$$k_z = \frac{\omega}{c} , \quad (37)$$

results in a real  $k_\Delta$  and an imaginary  $k_{\bar{\omega}_\theta}$ . In the other case (17) both  $k_\Delta$  and  $k_{\bar{\omega}_\theta}$  are real. The significance of this will become clear shortly.

The solution to (33) and (34) can be found by change of variables from  $r$  to  $k_\Delta r$  and  $k_{\bar{\omega}_\theta} r$  respectively. The resulting equations are Bessel equations of the zeroth and first orders respectively. The physically meaningful solutions which have bounded values at  $r = 0$ , are

$$\Delta(r, z, t) = G(z, t) J_0(k_\Delta r), \quad (38)$$

$$\bar{\omega}_\theta(r, z, t) = H(z, t) J_1(k_{\bar{\omega}_\theta} r), \quad (39)$$

where  $J_0(\cdot)$  and  $J_1(\cdot)$  are Bessel functions of the first kind and of zeroth and first orders respectively. Now the forms for the dilatation and rotation are given in (29) and (30). For these forms to match the solutions (38) and (39),  $U(r)$  and  $W(r)$  should have the following forms,

$$\begin{aligned} U(r) &= C_1 \frac{\partial}{\partial r} J_0(k_\Delta r) + C_2 k_z J_1(k_{\bar{\omega}_\theta} r) \\ &= -C_1 k_\Delta J_1(k_\Delta r) + C_2 k_z J_1(k_{\bar{\omega}_\theta} r), \end{aligned} \quad (40)$$

$$\begin{aligned} W(r) &= C_1 i k_z J_0(k_\Delta r) + C_2 \frac{i}{r} \frac{\partial}{\partial r} [r J_1(k_{\bar{\omega}_\theta} r)] \\ &= C_1 i k_z J_0(k_\Delta r) + C_2 i k_{\bar{\omega}_\theta} J_0(k_{\bar{\omega}_\theta} r), \end{aligned} \quad (41)$$

where  $C_1$  and  $C_2$  are two arbitrary constants. From (29) and (30) the dilatation and rotation become

$$\begin{aligned} \Delta(r, z, t) &= \\ &= -2C_1 (k_z^2 + k_\Delta^2) J_0(k_\Delta r) \exp(i(k_z z + \omega t)), \end{aligned} \quad (42)$$

$$\begin{aligned} 2\bar{\omega}_\theta(r, z, t) &= \\ &= 2iC_2 (k_z^2 + k_{\bar{\omega}_\theta}^2) J_1(k_{\bar{\omega}_\theta} r) \exp(i(k_z z + \omega t)). \end{aligned} \quad (43)$$

The wave can thus be a mixture of the longitudinal and shear components with  $C_1$  and  $C_2$  defining the respective proportions.

Now if  $k_\Delta$  is imaginary, the Bessel functions  $J_0(k_\Delta r)$  and  $J_1(k_\Delta r)$  go to infinity as  $r$  goes to infinity. This is not physically meaningful. Thus for a phase speed  $c$  which satisfies (16),

$C_1$  must be zero in (40) and (41). In view of (42) and (43) this is a purely shear wave beam, which travels at the phase speed  $c$ .

On the other hand if the phase speed  $c$  satisfies (17), both  $C_1$  and  $C_2$  can have nonzero values. Therefore infinitely many beam forms exist for which the wave travels at the phase speed  $c$ . Each of these beam forms contains both the longitudinal and shear components. This completes the proof.  $\square$

It follows that the phase speed depends not only on the mechanical properties of the medium, but also on the geometry of the wave. Even for a purely shear wave ( $C_1 = 0$ ), the phase speed can have any value which is greater than or equal to  $\sqrt{\mu/\rho}$ . *The shear wave speed,  $\sqrt{\mu/\rho}$ , is not the phase speed of every shear wave in an infinite medium.* It is however the phase speed of the uniform plane shear waves. This issue is in addition to the main drawback of the use of the phase speed<sup>63</sup> for tissue characterization; namely that the phase speed can not be defined when multiple waves are traveling in different directions, for instance when there are reflections of the wave from the boundaries.

## **B. Dependence of the Phase Speed on the Geometry of the Medium: Wave Guides**

In the previous section the medium was assumed to be infinite in size. This assumption is also made in many of the elastography techniques<sup>63,79</sup>. However no part of the human body is infinite in size. In this section we present some classical results on the wave guides and study their implications in the field of elastography. The wave guides are infinite in at least one direction and finite in at least another. Therefore they cannot model the tissue behavior accurately either. However they can be considered as an intermediate step in moving from the analysis of an infinite medium to a bounded medium. As such the insight gained from studying them is useful in understanding and designing elastography systems.

The wave guide we study is an infinitely long cylindrical rod. Choose the cylindrical coordinate system with the axis of the cylinder on the  $z$ -axis. As in the previous section,

we are interested in harmonic waves propagating along the  $z$ -axis, i.e. along the axis of the cylinder, which are symmetrical around the  $z$ -axis. The same analysis applies and the wave pattern given by (27) and (28) with  $U(r)$  and  $W(r)$  given by (40) and (41) satisfies the wave equation with phase speed  $c$ , provided that  $k_z$  is chosen to satisfy  $\omega/k_z = c$ . However in this case the boundary conditions impose restrictions on the permissible values of  $c$ .

The boundary of the cylinder is free from stresses. The expressions for stresses in the cylindrical coordinate system are,

$$\sigma_{rr} = \lambda\Delta + 2\mu\frac{\partial u_r}{\partial r}, \quad (44)$$

$$\sigma_{r\theta} = \mu \left[ \frac{1}{r} \frac{\partial u_r}{\partial \theta} + r \frac{\partial}{\partial r} \left( \frac{u_\theta}{r} \right) \right], \quad (45)$$

$$\sigma_{rz} = \mu \left[ \frac{\partial u_r}{\partial z} + \frac{\partial u_z}{\partial r} \right]. \quad (46)$$

By the assumptions  $\sigma_{r\theta}$  vanishes everywhere. The boundary conditions require that  $\sigma_{rr}$  and  $\sigma_{rz}$  vanish on the surface of the cylinder. Denote the radius of the cylinder by  $a$ . Substitution of the expressions for  $u_r$  and  $u_z$  from (27), (28), (40), and (41) translates the boundary conditions into the following two equations,

$$C_1 \left[ 2\mu \frac{\partial^2}{\partial r^2} \Big|_{r=a} J_0(k_\Delta r) - \frac{\lambda\rho\omega^2}{\lambda + 2\mu} J_0(k_\Delta a) \right] + 2C_2\mu k_z \frac{\partial}{\partial r} \Big|_{r=a} J_1(k_{\bar{\omega}_\theta} r) = 0, \quad (47)$$

$$2C_1 k_z \frac{\partial}{\partial r} \Big|_{r=a} J_0(k_\Delta r) + C_2 \left( 2k_z^2 - \frac{\rho\omega^2}{\mu} \right) J_1(k_{\bar{\omega}_\theta} a) = 0. \quad (48)$$

Note that these equations depend only on the ratio of  $C_1/C_2$ . Eliminating this variable between the two, a single equation is obtained for the unknown  $k_z$ . This equation is called the *Pochhammer frequency equation*<sup>62</sup>. For a given material  $\rho$ ,  $\mu$ ,  $\lambda$  and  $a$  are known. So the equation basically describes the relationship between the wave number  $k_z$  and angular frequency  $\omega$  of the wave, or equivalently the relationship between the phase speed  $c$  and  $\omega$ . As it turns out, unlike the infinite medium, not every phase speed is possible for a given  $\omega$ . The permissible speeds must satisfy the Pochhammer frequency equation. Substitution into

either of the equations (47) or (48) determines the ratio  $C_1/C_2$ , *i.e.* the proportions of the longitudinal and transversal waves that should be mixed together to obtain that particular phase speed.

## V. SIMULATION RESULTS

### A. Shear Waves in a Tissue Mimicking Infinite Medium

To gain some insight into the theoretical results which were presented in the previous section, we simulate the shear wave beam forms in an infinite medium for different angular frequencies and phase speeds. For a chosen pair of angular frequency  $\omega$  and phase speed  $c$ , the wave number  $k_z$  is found from (37). We choose the mechanical properties of the medium to match those found in the soft living tissue such as the breast. These values are listed in Table I. Given the mechanical properties of the medium,  $k_\Delta$  and  $k_{\bar{\omega}_\theta}$  are found from (35) and (36) respectively. In the next step  $U(r)$  and  $W(r)$  are found from (40) and (41), by setting  $C_1 = 0$  and choosing an arbitrary value for  $C_2$ . Note that  $C_1$  is chosen to be zero to obtain a purely shear wave and the value of  $C_2$  only determines the overall amplitude and phase of the wave, but does not change the waveform. If the time evolution of the wave is desired,  $U(r)$  and  $W(r)$  can be substituted in (27) and (28) to obtain  $u_r(r, z, t)$  and  $u_z(r, z, t)$ .

As shear waves can propagate at any phase speed above  $\sqrt{\mu/\rho} = \sqrt{10}\text{m/s}$ , the choice of the phase speed,  $c$ , becomes arbitrary. We simulated the beam forms using two chosen values of  $c = 5\text{m/s}$  and  $c = 12\text{m/s}$ . The results are shown in Fig. 1 and 2 respectively. The first and the second column in these figures show the displacement components  $u_r((r, \theta, z), t)$  and  $u_z((r, \theta, z), t)$  respectively at  $t = 0$ . The three rows correspond to increasing frequencies of the wave 40Hz, 65Hz, and 100Hz.

Note that because of the uniqueness of the solution to the wave equation, if a hypothetical planar exciter could be built which would create the same harmonic motion as  $u_r((r, \theta, z), t)$  and  $u_z((r, \theta, z), t)$  over an infinite cross section of the medium, for instance at  $z = 0$ , the wave forms due to this cylindrically symmetric infinite exciter, in the steady state, would be

the same as those depicted in these figures. The figures show how changing the excitation pattern of such an exciter can result in a completely different phase speed, even if the frequency of the excitation is not changed.

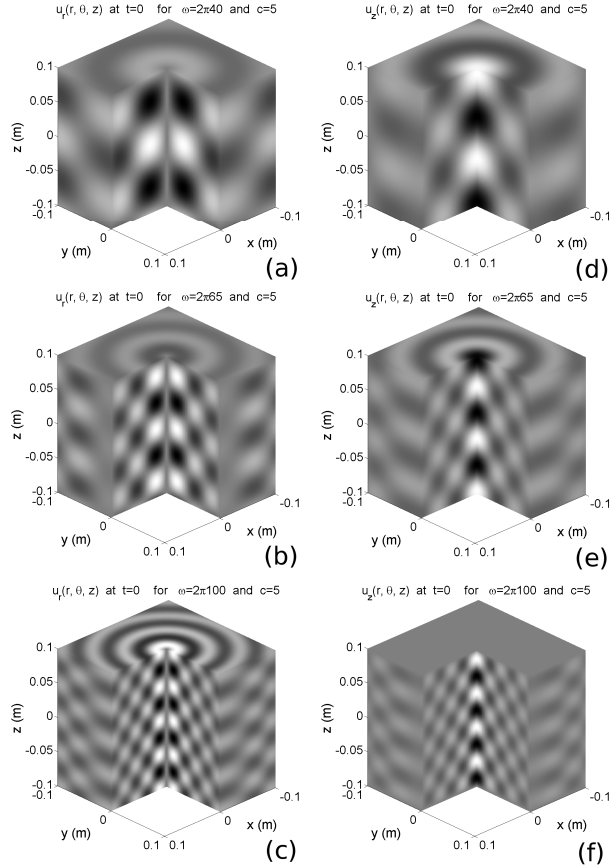


FIG. 1. Infinite medium; shear beam patterns for three different frequencies all sharing the same phase speed of 5m/s. (a), (b), (c) radial components of the displacement (d), (e), (f) z-component of the displacement at 40Hz, 65Hz, and 100Hz respectively. Note that only a cubic portion of the medium near the axis of symmetry is shown; The medium extends in all directions to infinity.

## B. Waves in a Tissue Mimicking Cylindrical Rod

The Pochhammer equation has been studied for metallic rods such as steel beams. To gain some insight into this equation when dealing with the living tissue, we consider a simple

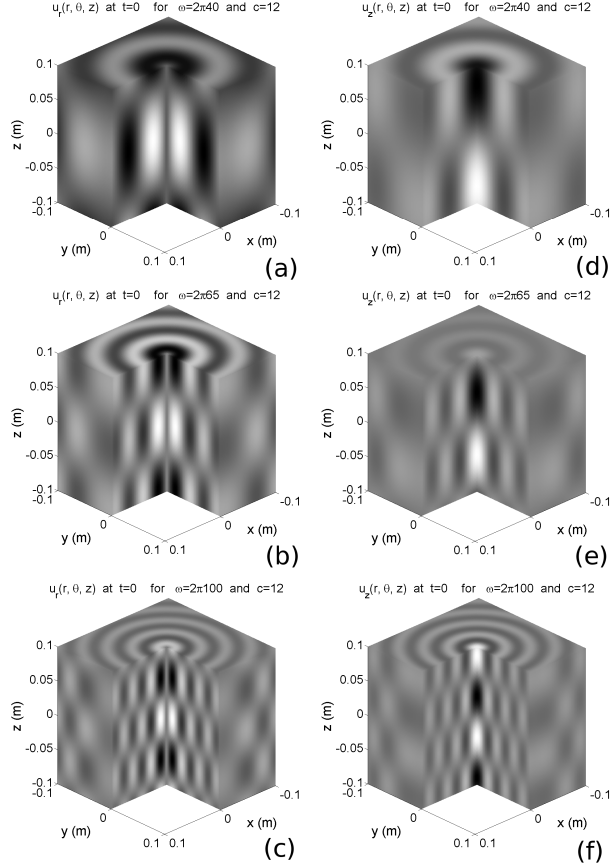


FIG. 2. Infinite medium; shear beam patterns for three different frequencies all sharing the same phase speed of 12m/s. (a), (b), (c) radial components of the displacement (d), (e), (f) z-component of the displacement at 40Hz, 65Hz, and 100Hz respectively. Note that only a cubic portion of the medium near the axis of symmetry is shown; The medium extends in all directions to infinity.

example here. We choose the mechanical properties of the medium to match those found in the living tissue. These values are listed in Table II. Using these values, the Pochhammer equation was solved numerically using MATLAB for different frequencies. Figure 3 shows the plots of the values of  $c$  obtained for each  $\omega$ . At higher frequencies, the equation has multiple roots (modes), thus the multiples plots in this figure.

Mode 0 has a constant phase speed  $c = \sqrt{\mu/\rho}$ , i.e. the shear wave speed for all frequencies. However substitution of the shear wave speed into (40) and (41) results in

$U(r) = W(r) = 0$ . Therefore this mode is a *trivial solution*. As a matter of fact assuming a phase speed equal to the shear wave speed results in vanishing displacements, independent of the material properties. The implication is that *no (axis symmetric) wave can travel along the cylindrical rod with the shear wave speed*.

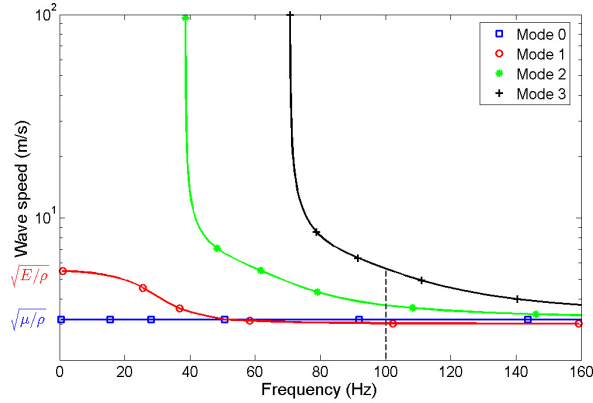


FIG. 3. The first four modes of the cylindrical bar

At low frequencies (below 38Hz) only mode 1 is present (see Fig. 3). Therefore the low frequency waves can only travel at a single speed. This is in contrast to the case of the infinite medium studied before, in which the waves, independent of their frequency, could travel at a range of speeds. The low frequency speed is equal to  $\sqrt{E/\rho}$  which is the familiar value obtained from the thin rod approximation theory<sup>64</sup>. This also shows the theoretical justification behind the assumptions made in (8). As the frequency goes higher, other modes start to appear.

At high frequencies (above 38Hz) multiple waves of the same frequency can propagate simultaneously, each with a different phase speed. For instance at a frequency of 100Hz, three phase speeds of 3.0339m/s, 3.719m/s, and 5.630m/s are possible. The corresponding beam patterns are shown in Fig. 4. In this case it may not be possible to recover a phase speed from studying the displacement patterns inside the material.

To see this more clearly, assume that a harmonic exciter vibrating at a frequency of

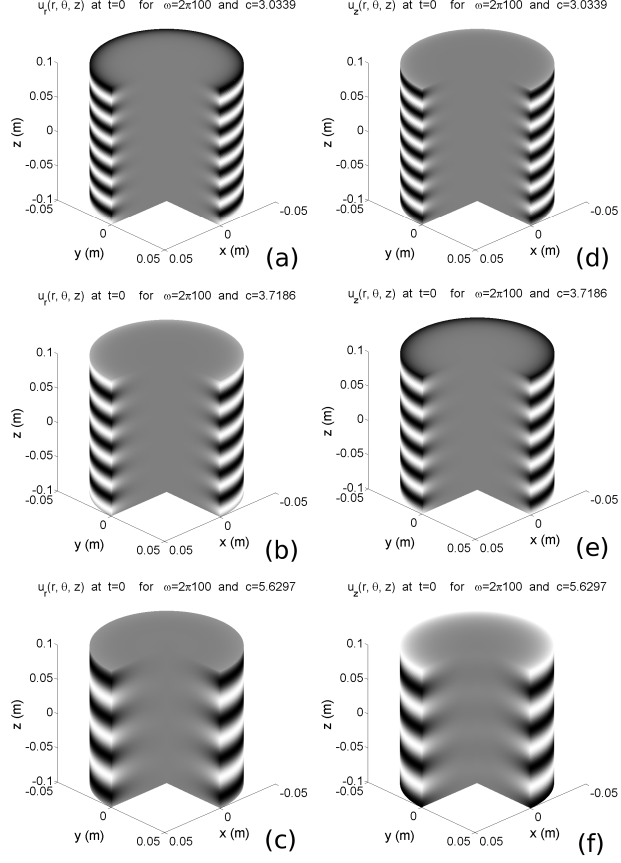


FIG. 4. Permissible beam patterns (modes) in an infinite cylindrical rod for waves having a frequency of 100Hz. Three (and only three) phase speeds are possible. (a), (b), (c) radial components of the displacement (d), (e), (f) z-component of the displacement for phase speeds of 3.0339m/s, 3.719m/s, and 5.630m/s respectively.

100Hz is placed at infinity on the rod and has caused the following wave pattern:

$$\begin{aligned}
 u_r(t) = & 3U_{c_1}(r) \exp(i(207.1z + 2\pi 100t)) \\
 & + 5U_{c_2}(r) \exp(i(168.94z + 2\pi 100t)) \\
 & + 8U_{c_3}(r) \exp(i(111.60z + 2\pi 100t)) , \tag{49}
 \end{aligned}$$

$$\begin{aligned}
 u_z(t) = & 3W_{c_1}(r) \exp(i(207.1z + 2\pi 100t)) \\
 & + 5W_{c_2}(r) \exp(i(168.94z + 2\pi 100t)) \\
 & + 8W_{c_3}(r) \exp(i(111.60z + 2\pi 100t)) , \tag{50}
 \end{aligned}$$

where the  $U_{c_i}$  and  $W_{c_i}$  are the solutions presented in Fig. 4 for the three phase speeds. Because of the linearity of the wave equation, any linear combination of the solutions presented in Fig. 4 is a solution. In particular the above linear combination with the coefficients 3, 5, and 8 caused by the particular exciter used, is a solution. It is not hard to verify by substitution that neither the direct inversion method (14), nor the phase gradient method (15) results in a meaningful mechanical property for the homogeneous cylinder.

The implication in the context of elastography is that at higher frequencies, multiple modes appear in the measured displacements which makes it impossible to recover a single phase speed and determine the mechanical properties based on that.

## VI. CONCLUSION

The propagation of elastic waves trapped in finite media, such as soft tissue, is a complex phenomenon even without considering the viscous and nonlinear effects. The term wave is generally applied to any vibration pattern inside the tissue. However the phase velocity cannot be defined for all the cases of the vibration patterns. Usually multiple waves traveling in different directions superimpose to create the vibration pattern. In this case the phase velocity might be well-defined for each wave, but not for the resultant of the superposition.

Even in the simple case where a single frequency wave is traveling in a single direction, the geometry of the wave and the medium create multiple permissible phase speeds, and thus make it difficult to recover a meaningful phase speed for the traveling wave. The parameters used in our simulations were chosen to be close to those of the living tissue. The diameter of the cylindrical rod was chosen to be 10cm which is in the same size range as human organs. Yet multiple phase speeds and modal behavior start to appear at frequencies as low as 38Hz. This frequency is in the range of frequencies used in many dynamic excitation elastography techniques.

One remedy seems to be the use of the natural decomposition of the vibrations into the longitudinal (dilatational) and transverse (shear) components. Each of these components

always satisfies its own wave equation with its own wave speed which is independent of the geometry (note that this is not the phase speed however). Taking the divergence of the measured displacement field yields the dilatation which satisfies the dilatational wave equation with wave speed  $\sqrt{(\lambda + 2\mu)/\rho}$ ,

$$\rho \frac{\partial^2 \Delta}{\partial t^2} = (\lambda + 2\mu) \nabla^2 \Delta. \quad (51)$$

Since living tissue is incompressible, the dilatations will be very minute and impossible to detect by taking the spatial derivatives of the measured displacements from any of the currently available imaging techniques. Even if accurate measurements were possible, inverting this wave equation would result in the local values of the longitudinal wave speed,  $\sqrt{(\lambda + 2\mu)/\rho}$ , being known. However the change of this parameter is quite small in the soft tissue (from 1400m/s for fat to 1540m/s for muscle). Therefore the contrast of the formed elastogram would be minimal.

On the other hand, taking the curl of the displacement field results in the rotation fields,

$$\nabla \times (u_x, u_y, u_z)^T = (\bar{\omega}_x, \bar{\omega}_y, \bar{\omega}_z)^T \quad (52)$$

each of which satisfies a shear wave equation with wave speed  $\sqrt{\mu/\rho}$ ,

$$\rho \frac{\partial^2 \bar{\omega}_i}{\partial t^2} = \mu \nabla^2 \bar{\omega}_i \quad i = x, y, z. \quad (53)$$

Since living tissue is incompressible,  $E \approx 3\mu$  and inverting these equations results in local information for tissue elasticity  $E$ . Moreover since these equations are naturally 1D, it is possible to use the phase speed in their context.

From this discussion it is concluded that *the only theoretically flawless method of imaging tissue elasticity is by taking the curl of the displacement fields*. This requires the measurement of the displacements in all three directions over the volume of interest. In cases where this is not feasible, such as ultrasound elastography, artifacts will always be present. These artifacts are not just due to noisy measurements, poor algorithms, or imperfect setups but due to the theoretical limitations of the systems themselves.

There are some measures which could be taken to minimize the artifacts. The main goal should be to create a single wave propagating in one direction at a single speed:

- The excitation amplitude should be chosen small enough to reduce the reflected wave amplitudes to the level of other measurement noises. The damping present in the tissue helps by reducing the amplitude of the reflected waves from the boundaries of the tissue and bones.
- The frequency of excitation should be kept to a minimum to prevent the appearance of higher modes. However lower frequencies result in lower damping, and therefore a trade off exists here.
- The excitation pattern should be chosen so as to excite mainly the lowest mode.

From an engineering point of view, however, many factors beyond the analysis presented here affect the success of an elastography system. Many of the devised elastography techniques are proven to provide clinically valuable images and some of them have even found their way into the market. Quasi-static constant strain, pulsed excitation with external exciters, acoustic-radiation-force-based and other techniques are each designed to make the displacements created in the clinical setting match the assumptions made about them. This results in the validity of their inversion techniques and their valuable elastograms.

The presence of the artifacts, by itself, does not mean that an elastography system should be dismissed. After all, each of the available medical imaging modalities has its own artifacts, and yet they are very well proven to be useful in diagnosis and treatment.

## **Acknowledgments**

This research was supported by the Canadian research funding agency NSERC.

## References

- <sup>1</sup> J. Ophir, I. Cespedes, H. Ponnekanti, Y. Yazdi, and X. Li, “Elastography: A quantitative method for imaging of elasticity of biological tissues”, *Ultrasonic Imaging* **13**, 111–134 (1991).
- <sup>2</sup> K. Parker, L. Gao, R. Lerner, and S. Levinson, “Techniques for elastic imaging: A review”, *IEEE Engineering in Medicine and Biology Magazine* **15**, 52–59 (1996).
- <sup>3</sup> L. Gao, K. J. Parker, R. M. Lerner, and S. Levinson, “Imaging of the elastic properties of tissue—a review”, *Ultrasound Med. Biol.* **22**, 957–977 (1996).
- <sup>4</sup> J. Ophir, B. Garra, F. Kallel, E. Konofagou, T. Krouskop, R. Righetti, and T. Varghese, “Elastographic imaging”, *Ultrasound Med. Biol.* **26**, S23–S29 (2000).
- <sup>5</sup> A. Sarvazyan, *Handbook of Elastic Properties of Solids, Liquids and Gases*, volume III, chapter Elastic Properties of Soft Tissues (Academic Press) (2001).
- <sup>6</sup> J. Ophir, S. K. Alam, B. Garra, F. Kallel, E. Konofagou, T. Krouskop, C. Merritt, R. Righetti, R. Souchon, S. Srinivasan, and T. Varghese, “Elastography: Imaging the elastic properties of soft tissues with ultrasound”, *Journal of Medical Ultrasonics* **29**, 155–171 (2002).
- <sup>7</sup> J. F. Greenleaf, M. Fatemi, and M. Insana, “Selected methods for imaging elastic properties of biological tissues”, *Annual Review Biomedical Engineering* **5**, 57–78 (2003).
- <sup>8</sup> K. J. Parker, L. S. Taylor, S. Gracewski, and D. J. Rubens, “A unified view of imaging the elastic properties of tissue”, *J. Acoust. Soc. Am.* **117**, 2705–2712 (2005).
- <sup>9</sup> T. Varghese, J. Ophir, and T. Krouskop, “Nonlinear stress-strain relationships in tissue and their effect on the contrast-to-noise ratio in elastograms”, *Ultrasound Med. Biol.* **26**, 839–851 (2000).
- <sup>10</sup> E. E. Konofagou, T. P. Harrigan, J. Ophir, and T. A. Krouskop, “Poroelastography: Imaging the poroelastic properties of tissues”, *Ultrasound Med. Biol.* **27**, 1387–1397 (2001).
- <sup>11</sup> S. Chen, M. Fatemi, and J. F. Greenleaf, “Quantifying elasticity and viscosity from mea-

- surement of shear wave speed dispersion”, *J. Acoust. Soc. Am.* **115**, 2781–2785 (2004).
- <sup>12</sup> J. Bercoff, M. Tanter, M. Muller, and M. Fink, “The role of viscosity in the impulse diffraction field of elastic waves induced by the acoustic radiation force”, *IEEE Trans. Ultrason. Ferroelect. Freq. Contr.* **51**, 1523–1536 (2004).
- <sup>13</sup> R. Righetti, J. Ophir, S. Srinivasan, and T. A. Krouskop, “The feasibility of using elastography for imaging the poisson’s ratio in porous media”, *Ultrasound Med. Biol.* **30**, 215–228 (2004).
- <sup>14</sup> R. Sinkus, M. Tanter, T. Xydeas, S. Catheline, J. Bercoff, and M. Fink, “Viscoelastic shear properties of in vivo breast lesions measured by mr elastography”, *Magnetic Resonance Imaging* **23**, 159–165 (2005).
- <sup>15</sup> R. Righetti, J. Ophir, and T. A. Krouskop, “A method for generating permeability elastograms and poisson’s ratio time-constant elastograms”, *Ultrasound Med. Biol.* **31**, 803–816 (2005).
- <sup>16</sup> S. Chen, R. Kinnick, J. F. Greenleaf, and M. Fatemi, “Difference frequency and its harmonic emitted by microbubbles under dual frequency excitation”, *Ultrasonics* **44**, 123–126 (2006).
- <sup>17</sup> R. Sinkus, J. Bercoff, M. Tanter, J.-L. Gennisson, C. E. Khoury, V. Servois, A. Tardivon, and M. Fink, “Nonlinear viscoelastic properties of tissue assessed by ultrasound”, *IEEE Trans. Ultrason. Ferroelect. Freq. Contr.* **53**, 2009–2018 (2006).
- <sup>18</sup> S. Chen, R. R. Kinnick, J. F. Greenleaf, and M. Fatemi, “Harmonic vibro-acoustography”, *IEEE Trans. Ultrason. Ferroelect. Freq. Contr.* **54**, 1346–1351 (2007).
- <sup>19</sup> X. Jacob, S. Catheline, J.-L. Gennisson, C. Barrière, D. Royer, and M. Fink, “Nonlinear shear wave interaction in soft solids”, *J. Acoust. Soc. Am.* **122**, 1917–1926 (2007).
- <sup>20</sup> A. Thitaikumar, T. A. Krouskop, B. S. Garra, and J. Ophir, “Visualization of bonding at an inclusion boundary using axial-shear strain elastography: a feasibility study”, *Phys. Med. Biol.* **52**, 2615–2633 (2007).
- <sup>21</sup> J. Gennisson, M. Rénier, S. Catheline, C. Barrière, J. Bercoff, M. Tanter, and M. Fink, “Acoustoelasticity in soft solids: Assessment of the nonlinear shear modulus with the

- acoustic radiation force”, *J. Acoust. Soc. Am.* **122**, 3211–3219 (2007).
- <sup>22</sup> A. Thitaikumar, L. M. Mobbs, C. M. Kraemer-Chant, B. S. Garra, and J. Ophir, “Breast tumor classification using axial shear strain elastography: a feasibility study”, *Phys. Med. Biol.* **53**, 4809–4823 (2008).
- <sup>23</sup> R. Lerner and K. Parker, “Sonoelasticity images, ultrasonic tissue characterization and echographic imaging”, in *Proceedings of the 7th European Communities Workshop* (1987), nijmegen, Netherlands.
- <sup>24</sup> R. Lerner, K. Parker, J. Holen, R. Gramiak, and R. Waag, “Sono-elasticity: Medical elasticity images derived from ultrasound signals in mechanically vibrated targets”, *Acoustical Imaging* **16**, 317–327 (1988).
- <sup>25</sup> R. Sinkus, J. Lorenzen, D. S. amd M. Lorenzen, M. Dargatz, and D. Holz, “High-resolution tensor mr elastography for breast tumor detection”, *Physics Med. Biol.* **45**, 1649–1664 (2000).
- <sup>26</sup> R. Souchon, L. Soualmi, M. Bertrand, J.-Y. Chapelon, F. Kallel, and J. Ophir, “Ultrasonic elastography using sector scan imaging and a radial compression”, *Ultrasonics* **40**, 867–871 (2002).
- <sup>27</sup> L. Sandrin, M. Tanter, S. Catheline, and M. Fink, “Shear modulus imaging with 2-d transient elastography”, *IEEE Trans. Ultrason. Ferroelect. Freq. Contr.* **49**, 426–435 (2002).
- <sup>28</sup> L. Sandrin, M. Tanter, J.-L. Gennisson, S. Catheline, and M. Fink, “Shear elasticity probe for soft tissues with 1-d transient elastography”, *IEEE Trans. Ultrason. Ferroelect. Freq. Contr.* **49**, 436–446 (2002).
- <sup>29</sup> J.-L. Gennisson, S. Catheline, S. Chaffai, and M. Fink, “Transient elastography in anisotropic medium: Application to the measurement of slow and fast shear wave speeds in muscles”, *J. Acoust. Soc. Am.* **114**, 536–541 (2003).
- <sup>30</sup> J. Bercoff, R. Sinkus, M. Tanter, and M. Fink, “Supersonic shear imaging: A new technique for soft tissue elasticity mapping”, *IEEE Trans. Ultrason. Ferroelect. Freq. Contr.* **51**, 396–409 (2004).

- <sup>31</sup> M. W. Urban and J. F. Greenleaf, “Harmonic pulsed excitation and motion detection of a vibrating reflective target”, *J. Acoust. Soc. Am.* **123**, 519–533 (2008).
- <sup>32</sup> F. Yeung, S. F. Levinson, D. Fu, and K. J. Parker, “Feature-adaptive motion tracking of ultrasound image sequences using a deformable mesh”, *IEEE Trans. Med. Imaging* **17**, 945–956 (1998).
- <sup>33</sup> E. Konofagou, T. Varghese, J. Ophir, and S. Alam, “Power spectral strain estimators in elastography”, *Ultrasound Med. Biol.* **25**, 1115–1129 (1999).
- <sup>34</sup> E. E. Konofagou and J. Ophir, “Precision estimation and imaging of normal and shear components of the 3d strain tensor in elastography”, *Phys. Med. Biol.* **45**, 1553–1563 (2000).
- <sup>35</sup> T. Varghese, E. Konofagou, J. Ophir, S. Alam, and M. Bilgen, “Direct strain estimation in elastography using spectral cross-correlation”, *Ultrasound Med. Biol.* **26**, 1525–1537 (2000).
- <sup>36</sup> M. Fink, L. Sandrin, M. Tanter, S. Catheline, S. Chaffai, J. Bercoff, and J. Gennisson, “Ultra high speed imaging of elasticity”, in *IEEE Ultrasonics Symposium*, 1811–1820 (2002).
- <sup>37</sup> J. Bercoff, R. Sinkus, M. Tanter, and M. Fink, “3d ultrasound-based dynamic and transient elastography: First in vitro results”, in *IEEE Ultrasonics Symposium*, 28–31 (2004).
- <sup>38</sup> K. Hoyt, F. Forsberg, and J. Ophir, “Investigation of parametric spectral estimation techniques for elasticity imaging”, *Ultrasound Med. Biol.* **31**, 1109–1121 (2005).
- <sup>39</sup> K. Hoyt, F. Forsberg, and J. Ophir, “Comparison of shift estimation strategies in spectral elastography”, *Ultrasonics* **44**, 99–108 (2006).
- <sup>40</sup> K. Hoyt, F. Forsberg, and J. Ophir, “Analysis of a hybrid spectral strain estimation technique in elastography”, *Phys. Med. Biol.* **51**, 197–209 (2006).
- <sup>41</sup> J.-L. Gennisson, T. Defieux, R. Sinkus, P. Annic, M. Pernot, F. Cudeiro, G. Montaldo, M. Tanter, M. Fink, and J. Bercoff, “A 3d elastography system based on the concept of ultrasound-computed tomography for in vivo breast examination”, in *IEEE Ultrasonics*

- Symposium*, 1037–1040 (2006).
- <sup>42</sup> A. J. Romano, J. J. Shirron, and J. A. Bucaro, “On the noninvasive determination of material parameters from a knowledge of elastic displacements: Theory and numerical simulation”, *IEEE Trans. Ultrason. Ferroelect. Freq. Contr.* **45**, 751–759 (1998).
- <sup>43</sup> C. Sumi, A. Suzuki, and K. Nakayama, “Estimation of shear modulus distribution in soft tissue from strain distribution”, *IEEE Trans. Biomed. Eng.* **42**, 193–202 (1995).
- <sup>44</sup> K. Raghavan and A. E. Yagle, “Forward and inverse problems in elasticity imaging of soft tissues”, *IEEE Transactions on Nuclear Science* **41**, 1639–1648 (1994).
- <sup>45</sup> F. Kallel and M. Bertrand, “Tissue elasticity reconstruction using linear perturbation method”, *IEEE Trans. Med. Imaging* **15**, 299–313 (1996).
- <sup>46</sup> M. Doyley, P. Meaney, and J. Bamber, “Evaluation of an iterative reconstruction method for quantitative elastography”, *Phys. Med. Biol.* **45**, 1521–1540 (2000).
- <sup>47</sup> P. E. Barbone and J. C. Bamber, “Quantitative elasticity imaging: What can and cannot be inferred from strain images”, *Phys. Med. Biol.* **47**, 2147–2164 (2002).
- <sup>48</sup> A. A. Oberai, N. H. Gokhale, and G. R. Feijóo, “Solution of inverse problems in elasticity imaging using the adjoint method”, *Inverse Problems* **19**, 297–313 (2003).
- <sup>49</sup> D. Fu, S. Levinson, S. Gracewski, and K. Parker, “Non-invasive quantitative reconstruction of tissue elasticity using an iterative forward approach”, *Phys. Med. Biol.* **45** (2000) 1495–1509 **45**, 1495–1509 (2000).
- <sup>50</sup> A. Manduca, T. Oliphant, M. Dresner, J. Mahowald, S. Kruse, E. Amromin, J. Felmlee, J. Greenleaf, and R. Ehman, “Magnetic resonance elastography: Non-invasive mapping of tissue elasticity”, *Medical Image Analysis* **5**, 237–2540 (2001).
- <sup>51</sup> T. Oliphant, A. Manduca, R. Ehman, and J. Greenleaf, “Complex-valued stiffness reconstruction by for magnetic resonance elastography by algebraic inversion of the differential equation”, *Magnetic Resonance in Medicine* **45**, 299–310 (2001).
- <sup>52</sup> S. Catheline, J. Gennisson, G. Delon, M. Fink, R. Sinkus, S. Abouelkaram, and J. Culiolic, “Measurement of viscoelastic properties of homogeneous soft solid using transient elastography: An inverse problem approach”, *J. Acoust. Soc. Am.* **116**, 3734–3741 (2004).

- <sup>53</sup> B. Robert, R. Sinkus, B. Larrat, M. Tanter, and M. Fink, “A new rheological model based on fractional derivatives for biological tissues”, in *IEEE Ultrasonics Symposium*, 1033–1036 (2006).
- <sup>54</sup> X. Zhang and J. F. Greenleaf, “Estimation of tissues elasticity with surface wave speed (I)”, *J. Acoust. Soc. Am.* **122**, 2522–2525 (2007).
- <sup>55</sup> A. A. Oberai, N. H. Gokhale, M. M. Doyley, and J. C. Bamber, “Evaluation of the adjoint equation based algorithm for elasticity imaging”, *Phys. Med. Biol.* **49**, 2955–2974 (2004).
- <sup>56</sup> M. M. Doyley, S. Srinivasan, S. A. Pendergrass, Z. Wu, and J. Ophir, “Comparative evaluation of strain-based and model-based modulus elastography”, *Ultrasound Med. Biol.* **31**, 787–802 (2005).
- <sup>57</sup> M. M. Doyley, S. Srinivasan, E. Dimidenko, N. Soni, and J. Ophir, “Enhancing the performance of model-based elastography by incorporating additional a priori information in the modulus image reconstruction process”, *Phys. Med. Biol.* **51**, 95–112 (2006).
- <sup>58</sup> J. Bercoff, S. Chaffai, M. Tanter, L. Sandrin, S. Catheline, M. Fink, J. L. Gennisson, and M. Meunier, “In vivo breast tumor detection using transient elastography”, *Magnetic Resonance in Medicine* **29**, 1387–1396 (2003).
- <sup>59</sup> J. Bercoff, M. Muller, M. Tanter, and M. Fink, “Study of viscous and elastic properties of soft tissue using supersonic shear imaging”, in *IEEE Ultrasonics Symposium*, 925–928 (2003).
- <sup>60</sup> J. Fromageau, J.-L. Gennisson, C. Schmitt, R. L. Maurice, R. Mongrain, and G. Cloutier, “Estimation of polyvinyl alcohol cryogel mechanical properties with four ultrasound elastography methods and comparison with gold standard testing”, *IEEE Trans. Ultrason. Ferroelect. Freq. Contr.* **54**, 498–509 (2007).
- <sup>61</sup> A. Romano, J. Bucaro, P. Abraham, and S. Dey, “Inversion methods for the detection and localization of inclusions in structures utilizing dynamic surface displacements”, in *Proceedings of SPIE Vol. 5503*, volume 5503, 367–374 (2004).
- <sup>62</sup> H. Kolsky, *Stress Waves in Solids* (Dover Publications, Inc., New York) (1963).
- <sup>63</sup> S. Catheline, F. Wu, and M. Fink, “A solution to diffraction biases in sonoelasticity: The

- acoustic impulse technique”, *J. Acoust. Soc. Am.* **105** (1999).
- <sup>64</sup> A. Baghani, H. Eskandari, T. Salcudean, and R. Rohling, “Measurement of tissue elasticity using longitudinal waves”, in *Proceedings of the 7th International conference on the Ultrasonic Measurement and Imaging of Tissue Elasticity*, 103 (2008).
- <sup>65</sup> F. A. Duck, *Physical Properties of Tissue: A Comprehensive Reference Book* (Academic Press) (1990).
- <sup>66</sup> M. M. Burlaw, E. L. Madsen, J. A. Zagzebski, R. A. Bahjovic, and S. W. Sum, “A new ultrasound tissue-equivalent material”, *Radiology* **134**, 517–520 (1980).
- <sup>67</sup> S. A. Goss, R. L. Johnston, and F. Dunn, “Comprehensive compilation of empirical ultrasonic properties of mammalian tissues”, *J. Acoust. Soc. Am.* **64**, 423–457 (1978).
- <sup>68</sup> A. Sarvazyan, O. Rudenko, S. Swanson, J. Fowlkes, and S. Emelianov, “Shear wave elasticity imaging: A new ultrasonic technology of medical diagnostics”, *Ultrasound Med. Biol.* **24**, 1419–1435 (1998).
- <sup>69</sup> M. Walz, J. Teubner, and M. Georgi, “Elasticity of benign and malignant breast lesions”, in *Imaging, Application and Results in Clinical and General Practice*, 56 (1993), eight International Congress on the Ultrasonic Examination of the Breast.
- <sup>70</sup> W.-C. Yeh, P.-C. Li, Y.-M. J. amd Hey-Chi Hsu, P.-L. Kuo, M.-L. Li, P.-M. Yang, and P. H. Lee, “Elastic modulus measurements of human liver and correlation with pathology”, *Ultrasound Med. Biol.* **28**, 467–474 (2002).
- <sup>71</sup> T. Krouskop, T. Wheeler, F. Kallel, B. Garra, and T. Hall, “Elastic moduli of breast and prostate tissues under compression”, *Ultrasonic Imaging* **20**, 260–274 (1998).
- <sup>72</sup> M. Muller, J.-L. Gennisson, T. Deffieux, R. Sinkus, P. Annic, G. Montaldo, M. Tanter, and M. Fink, “Full 3d inversion of the viscoelasticity wave propagation problem for 3d ultrasound elastography in breast cancer diagnosis”, in *IEEE Ultrasonics Symposium*, 672–675 (2007).
- <sup>73</sup> L. Huwart, F. Peeters, R. Sinkus, L. Annet, N. Salameh, L. C. ter Beek, Y. Horsmans, and B. E. V. Beers, “Liver fibrosis: Non-invasive assessment with mr elastography”, *NMR in Biomedicine* **19**, 173–179 (2006).

- <sup>74</sup> R. Sinkus, M. Tanter, S. Catheline, J. Lorenzen, C. Kuhl, E. Sondermann, and M. Fink, “Imaging anisotropic and viscous properties of breast tissue by magnetic resonance-elastography”, *Magnetic Resonance in Medicine* **53**, 372–387 (2005).
- <sup>75</sup> R. Sinkus, K. Siegmann, T. Xydeas, M. Tanter, C. Claussen, and M. Fink, “Mr elastography of breast lesions: Understanding the solid/liquid duality can improve the specificity of contrast-enhanced mr mammography”, *Magnetic Resonance in Medicine* **58**, 1135–1144 (2007).
- <sup>76</sup> R. Baierlein, “Representing a vector field: Helmholtz’s theorem derived from a fourier identity”, *Am. J. Phys.* **63**, 180–182 (1995).
- <sup>77</sup> F. Rohrlich, “Causality, the coulomb field, and newton’s law of gravitation”, *Am. J. Phys.* **70**, 411–414 (2002).
- <sup>78</sup> K. F. Graff, *Wave Motion in Elastic Solids* (Oxford University Press, Ely House, London) (1975).
- <sup>79</sup> L. Sandrin, D. Cassereau, and M. Fink, “The role of the coupling term in transient elastography”, *J. Acoust. Soc. Am.* **115**, 73–83 (2004).

TABLE I. Mechanical property values used for the simulation

$\rho$	$\lambda$	$\mu$
kg/m <sup>3</sup>	GPa	kPa
1000	2.3	10

TABLE II. Mechanical property values used for the simulation

$\rho$	$\lambda$	$\mu$	$a$
kg/m <sup>3</sup>	GPa	kPa	m
1000	2.3	10	0.05

**List of Figures**

FIG. 1 Infinite medium; shear beam patterns for three different frequencies all sharing the same phase speed of 5m/s. (a), (b), (c) radial components of the displacement (d), (e), (f) z-component of the displacement at 40Hz, 65Hz, and 100Hz respectively. Note that only a cubic portion of the medium near the axis of symmetry is shown; The medium extends in all directions to infinity. 19

FIG. 2 Infinite medium; shear beam patterns for three different frequencies all sharing the same phase speed of 12m/s. (a), (b), (c) radial components of the displacement (d), (e), (f) z-component of the displacement at 40Hz, 65Hz, and 100Hz respectively. Note that only a cubic portion of the medium near the axis of symmetry is shown; The medium extends in all directions to infinity. 20

FIG. 3 The first four modes of the cylindrical bar . . . . . 21

FIG. 4 Permissible beam patterns (modes) in an infinite cylindrical rod for waves having a frequency of 100Hz. Three (and only three) phase speeds are possible. (a), (b), (c) radial components of the displacement (d), (e), (f) z-component of the displacement for phase speeds of 3.0339m/s, 3.719m/s, and 5.630m/s respectively. . . . . 22